Comparison of Engineer's and Astronomical Noise Diode Values For Four Receivers

C. Johnson, R. Maddalena, F. Ghigo, and D. Balser
December 3, 2002

Abstract

Using GBT data collected from the 1-2 GHz, 2-3 GHz, 4-6 GHz, and 8-10 GHz receivers, comparisons were made between the observed and the engineer's values for the noise diode intensity, T_{cal}. With few exceptions, the values agreed. We believe that our T_{cal} values are accurate to about 1% in comparison to those determined by the engineers, whose intrinsic accuracies are about 5%.

A. Introduction

In this memo, we will compare the engineers' noise diode temperature values with the astronomically determined values for each of four receivers. Linear and circular polarization values were compared using the 1-2 GHz and 2-3 GHz receivers, linear using the 4-6 GHz receiver and circular using the 8-10 GHz receiver.

Table 1 outlines the continuum calibration source and date for each astronomical observation. Table 2 outlines the calibration parameters for the engineer's values.

Table 1. Astronomical measurements.

Receiver	Calibration source	Date	Observer(s)
1-2 GHz	3C295	31 July 2002	Roberts, Maddalena, Haynes, Hogg
	3C348	31 July - 04 Aug 2002	Roberts, Maddalena, Haynes, Hogg
	3C48	03 Aug 2002	Roberts, Maddalena, Haynes, Hogg
	3C147	03-04 Aug 2002	Roberts, Maddalena, Haynes, Hogg
	3C161	03-04 Aug 2002	Roberts, Maddalena, Haynes, Hogg
	3C147	11 Aug 2002	Maddalena & Johnson
2-3 GHz	3C147	18 May 2002	Maddalena
4-6 GHz	3C286	24 Apr 2002	Balser
8-10 GHz	3C286	22 May 2002	Ghigo

Table 2. Engineer's measurements.

Receiver	T hot	T cold	Date	Engineer	Bandwidth
1-2 GHz	285.0 K	5.0 K	14 Feb 2002	Stennes	2 MHz
2-3 GHz	295.0 K	6.0 K	19 Sep 2001	Stennes	2 MHz
4-6 GHz	298.0 K	80.0 K	05 Mar 2002	Simon	20 MHz
8-10 GHz	300.0 K	82.0 K	16 Jul 2001	Stennes	20 MHz

Using the Spectral Processor, data were collected in the Off-On, Total Power observing mode. The scans were spaced 30 MHz apart but the bandwidth of each scan was 40 MHz. Therefore, there was an overlap of 10 MHz for each successive observation. We spent one minute on source and one minute off source.

Each observation has 1024 channels. Pointing was done beforehand to ensure that we were aimed directly at the calibration source. Typically one complete bandpass of a receiver can be measured within a couple of hours.

B. Calculations

The source temperature as a function of frequency, $T_{src}(\nu)$, can be calculated by knowing the flux density, $S(\nu)$, and the efficiency, η, of the antenna:

$$T_{src}(\nu) = [Area / 2k] * S(\nu) * \eta * e^{-\tau A},$$

where τ is the opacity of the atmosphere at the time of observation and $A = 1/\sin(elevation)$. For the GBT, this equation is:

$$T_{src}(\nu) = 2.84 * S(\nu) * \eta * e^{-\tau A}. \qquad (1)$$

If we define:

P_{sig}^{on} as the power with the noise diode on when the telescope is pointed on the source,
P_{sig}^{off} as the power with the noise diode off when the telescope is pointed on the source,
P_{ref}^{on} as the power with the noise diode on when the telescope is pointed off the source,
P_{ref}^{off} as the power with the noise diode off when the telescope is pointed off the source,

$$P_{sig}(\nu) = \frac{P_{sig}^{on}(\nu) + P_{sig}^{off}(\nu)}{2},$$

$$P_{ref}(\nu) = \frac{P_{ref}^{on}(\nu) + P_{ref}^{off}(\nu)}{2},$$

and if we assume a linear system, then

$$T_{src}(\nu) = \left\langle \frac{P_{sig}(\nu) - P_{ref}(\nu)}{P_{ref}^{on}(\nu) - P_{ref}^{off}(\nu)} \right\rangle_{1MHz} * T_{cal}(\nu) \qquad (2)$$

$$S(\nu) = \left\langle \frac{P_{sig}(\nu) - P_{ref}(\nu)}{P_{ref}^{on}(\nu) - P_{ref}^{off}(\nu)} \right\rangle_{1MHz} * S_{cal}(\nu)$$

where $\left\langle \frac{P_{sig}(\nu) - P_{ref}(\nu)}{P^{on}_{ref}(\nu) - P^{off}_{ref}(\nu)} \right\rangle_{1MHz}$ denotes an average over 25 channels, or 0.976 MHz.

Combining equation (1) with equation (2), and solving for T_{cal} and S_{cal}, gives:

$$T^{ast}_{cal}(\nu) = 2.84 * S(\nu) * \eta * e^{-\tau A} * \left\langle \frac{P^{on}_{ref}(\nu) - P^{off}_{ref}(\nu)}{P_{sig}(\nu) - P_{ref}(\nu)} \right\rangle_{1Mhz}$$

$$S^{ast}_{cal}(\nu) = S(\nu) * e^{\tau A} * \left\langle \frac{P^{on}_{ref}(\nu) - P^{off}_{ref}(\nu)}{P_{sig}(\nu) - P_{ref}(\nu)} \right\rangle_{1MHz} .$$

Note that $\frac{S_{cal}}{T_{cal}} = 2.84 * \eta$. AIPS++ and the glish script given in the Appendix were used to calculate $\left\langle \frac{P^{on}_{ref}(\nu) - P^{off}_{ref}(\nu)}{P_{sig}(\nu) - P_{ref}(\nu)} \right\rangle$.

For each scan, the data were exported into a text editor, then to a PSI-plot data sheet, and finally into one comprehensive data file. The first five and last five channels for each scan were deleted from the final data file since edge channels inherently cannot be calibrated.

In order to calculate the flux density (S) for each frequency for known calibration sources, we consulted *Ott, et al (1993)*. In that paper, *Ott et al* provide the coefficients of second-order polynomials in $\log S$ as a function of $\log \nu$.

C. Error Analysis

We estimated that our random errors are about 0.25% as determined from the radiometer equation. Systematic errors may come from any of the following:

- Pointing. A pointing error would reduce P_{sig}-P_{ref} causing a systematic overestimation of $T^{AST}_{CAL}(\nu)$. A pointing error of 6.0% of the beamwidth would produce a 1% overestimate of T_{cal}.
- Efficiency. We have assumed that η=69% for all calculations. (It is necessary to note that $S_{cal}(\nu)$ is derived without any assumptions of efficiency.) $T^{AST}_{CAL}(\nu)$ and η can not be determined independently from astronomical observations. Therefore, an error in our assumed efficiencies will result in a systematic scaling of our $T^{AST}_{CAL}(\nu)$ values.
- Polarization. The data were not corrected for intrinsic source polarization. Only the data for 3C161 at 1-2 GHz might have introduced, at most, a 3% systematic error. For all other sources, the correction for polarization would have been less than 1%.
- Source size. Only 3C348 data needed to be adjusted for source size.
- Source fluxes. The *Ott, et al* values of $S(\nu)$ are precise to about 5%.

- Opacities. It is often difficult to determine the exact opacity of the atmosphere during an observation. Opacity may also change over the duration of an observation.

It is also noteworthy that the graphs of the engineer's values, $T_{CAL}^{ENG}(\nu)$ are not as smooth as the astronomical data due to fewer readings taken across the receiver's bandpass and higher random and systematic errors. There are five main sources of errors in the engineer's values:

- Uncertainty in the effective blackbody temperatures. To have a perfect blackbody calibrator, it must be a perfect radiator at all frequencies, and we must know its physical temperature very accurately. Typically, the engineers can measure physical temperature to within 0.1 K, but the engineer's thermometer is not calibrated. Also, the blackbody calibrators are not perfect radiators at all frequencies.
- The T_{cal} level will change with the temperature of the surrounding air. So, if the engineers manage to achieve 1% accuracy in the lab, it may be spoiled when the receiver is put on the telescope, where the ambient temperature might be different.
- Unstable receiver gain. This is usually a very small effect, as long as the engineer's measurements are taken over a short period of time. Typically, $\frac{\Delta G}{G} < 10^{-4}$.
- Uncertainty in the power measurements. This is probably the smallest error. The engineer's do not actually use absolute power readings in their calculations, but power ratios, which tend to be more accurate.
- Poorly matched blackbody calibrators. These introduce another level of uncertainty, as they will affect in the noise temperature and gain of the receiver. This may be a strong or a weak effect, depending on the amplifier's sensitivity to embedding (source) impedance. Most likely, this error is on the order of 1-2%.
- Uncertainty in sky brightness when the sky is used as a cold load.

D. 1 - 2 GHz Receiver

Significant interference from satellites (esp., GLONASS and GPS), aircraft warning systems (TCAS), and miscellaneous RFI spikes resulted in unusable data below 1300 MHz (Figures 1 – 4). There was also a mysterious feature observed at 1448 MHz that may be due to RFI or a receiver "suck out." The rest of the band had reasonable levels of RFI, though wherever RFI existed a spike can be seen on the graph. On the higher end of the 1-2 GHz receiver data, astronomical and engineer's calibration values are quite similar as seen.

Figure 1. X-Linear Polarization for 1-2 GHz Receiver.

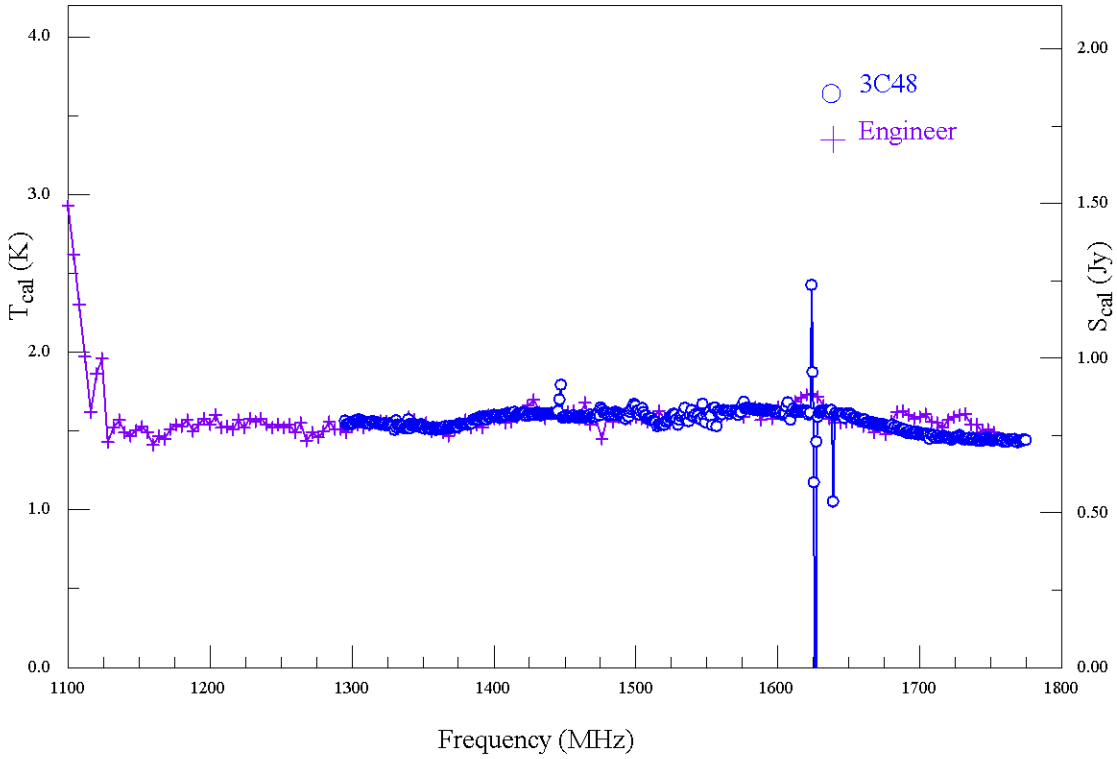

Figure 2. Y-Linear Polarization for 1-2 GHz Receiver.

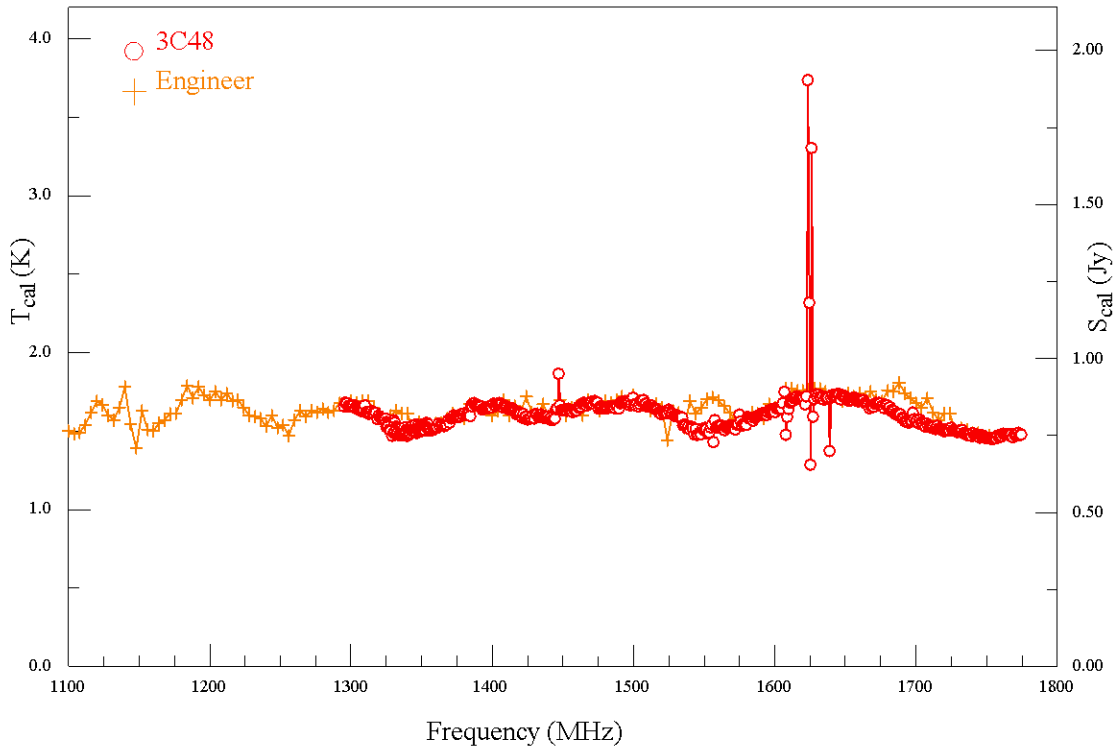

Figure 3. Left-Circular Polarization for the 1-2 GHz Receiver.

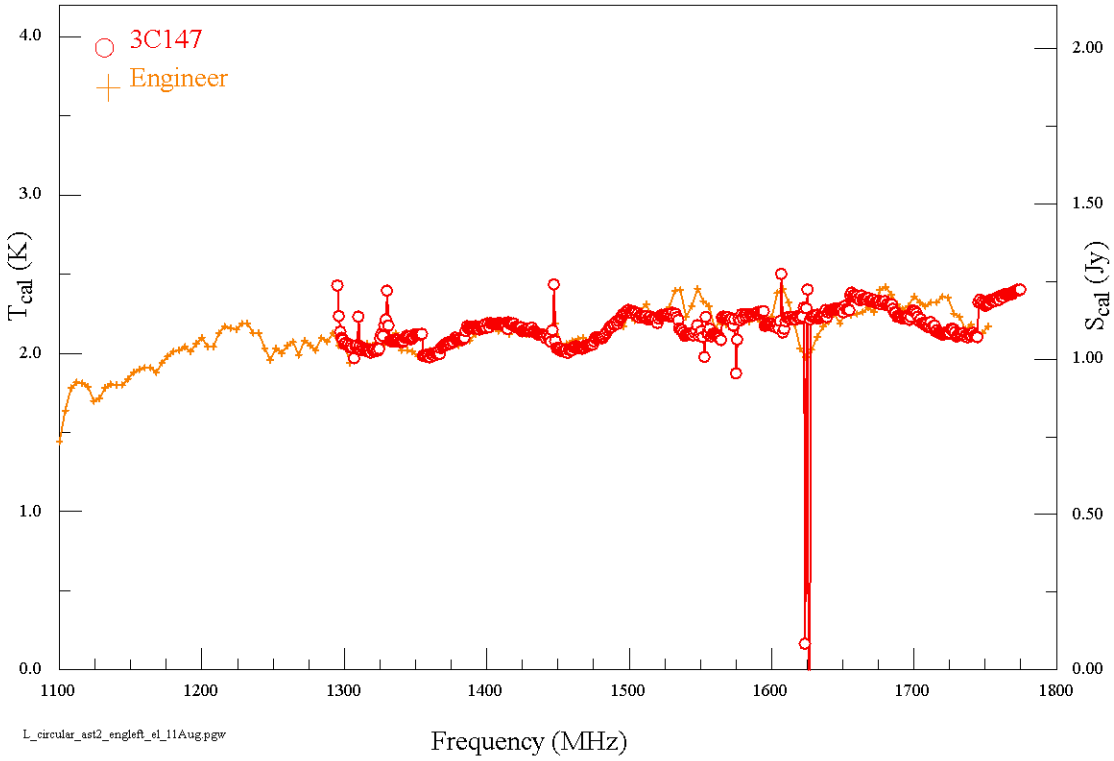

Figure 4. Right-Circular Polarization for the 1-2 GHz Receiver.

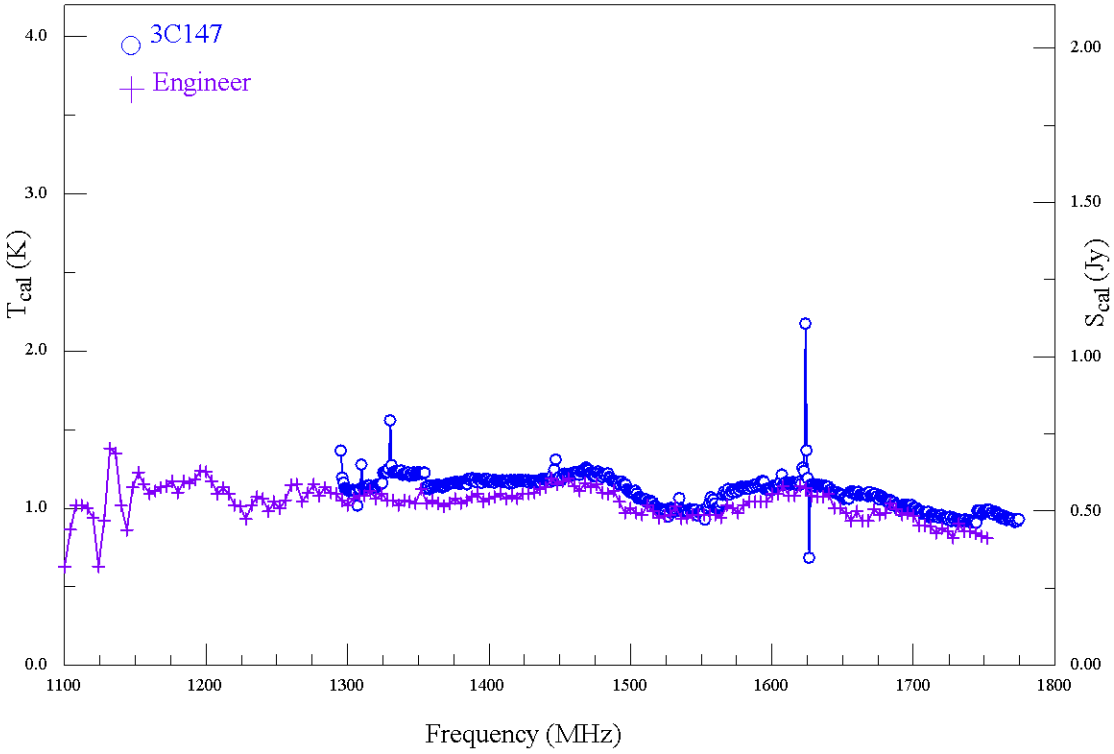

To assess the systematic errors in our method and to assist with the calibration of the *Roberts, et al* experiment, we repeated the linear-polarization calibration of the 1-2 GHz

receiver using a 40-MHz bandwidth for multiple calibrators multiple times. These results are shown in figures 5 and 6.

Two major conclusions can be drawn from these graphs:

- 3C161, since we have not compensated for its polarization, may have as much as a 3% systematic error. All other sources are consistent to within 3%.
- Repeated observations of the same source were typically within 1%.

Figure 5. X-Linear Polarization for a section of 1-2 GHz receiver used during Roberts et al.

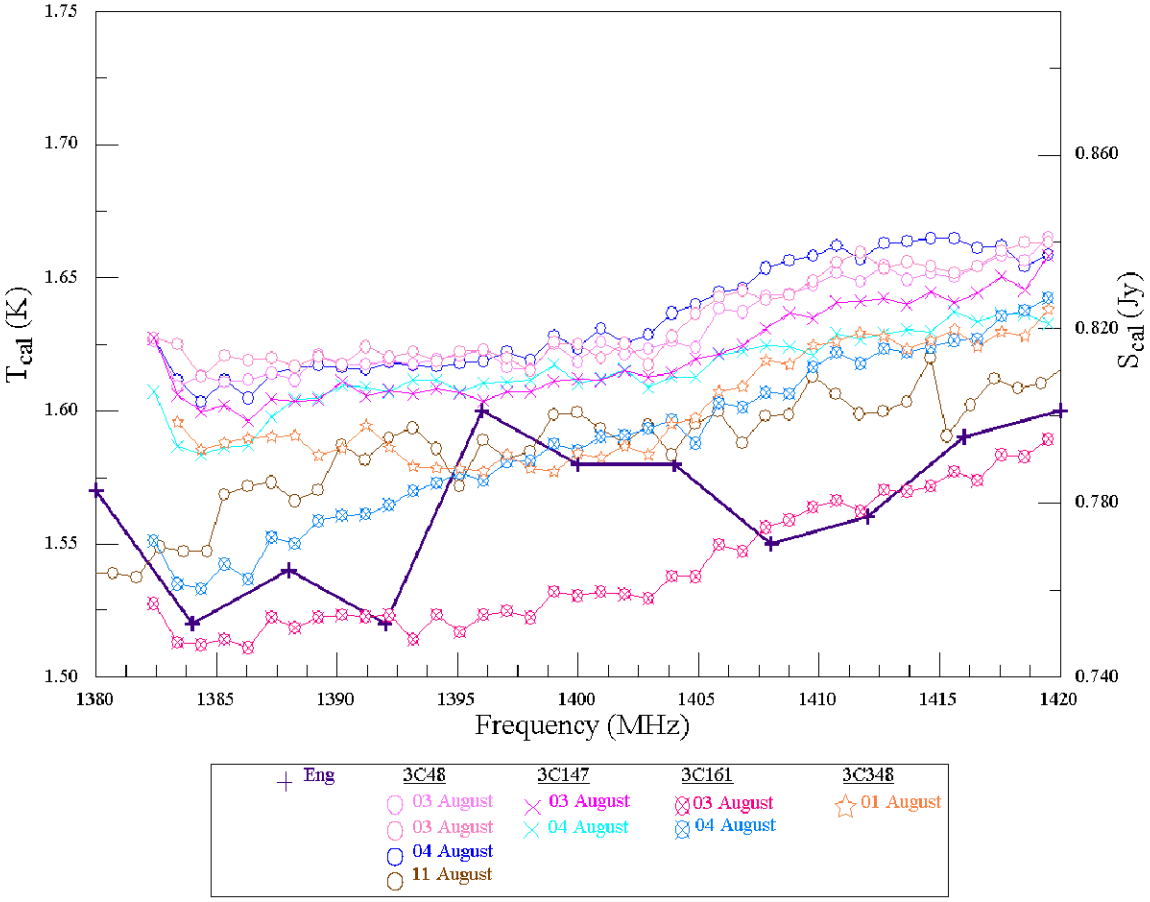

Figure 6. Y-Linear Polarization for a section of 1-2 GHz receiver used during Roberts et al.

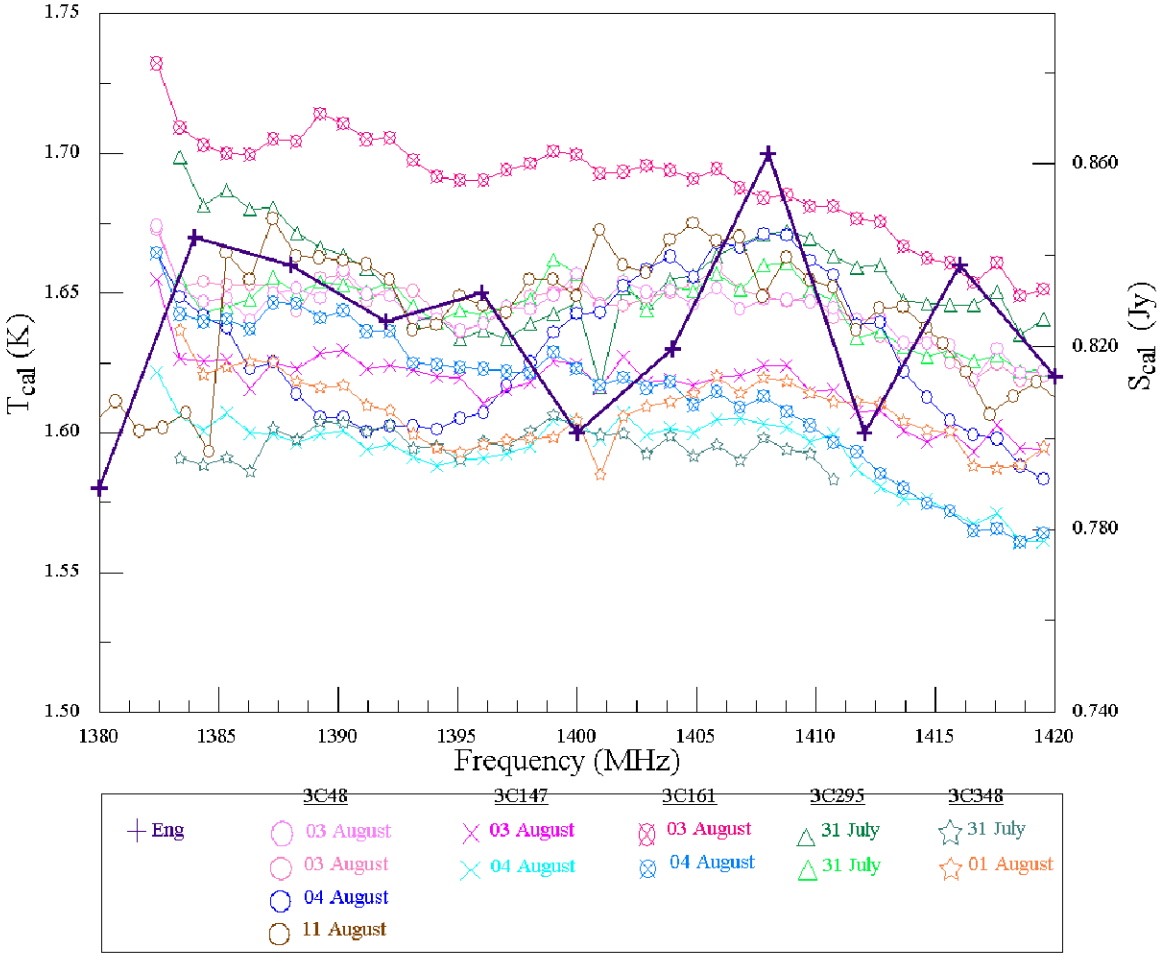

E. 2 – 3 GHz Receiver

Although the linear polarization data for the 2-3 GHz receiver show similar slopes as seen in figures 7 and 8, the engineer's values almost always are lower than the astronomical values. At the low end of the receiver's band, the values are quite similar, but noticeable differences can be seen as the frequency increases. The slope of the astronomical values is greater than the slope of the engineer's values. As seen in figures 9 and 10, circular polarization values, for the most part, also agree

Overall, the engineer's values seem to bounce around significantly more than the astronomical values. Significant RFI spikes occurred in the 2320 – 2350 range due to communication and entertainment satellites.

Figure 7. X-Linear Polarization for the 2-3 GHz Receiver.

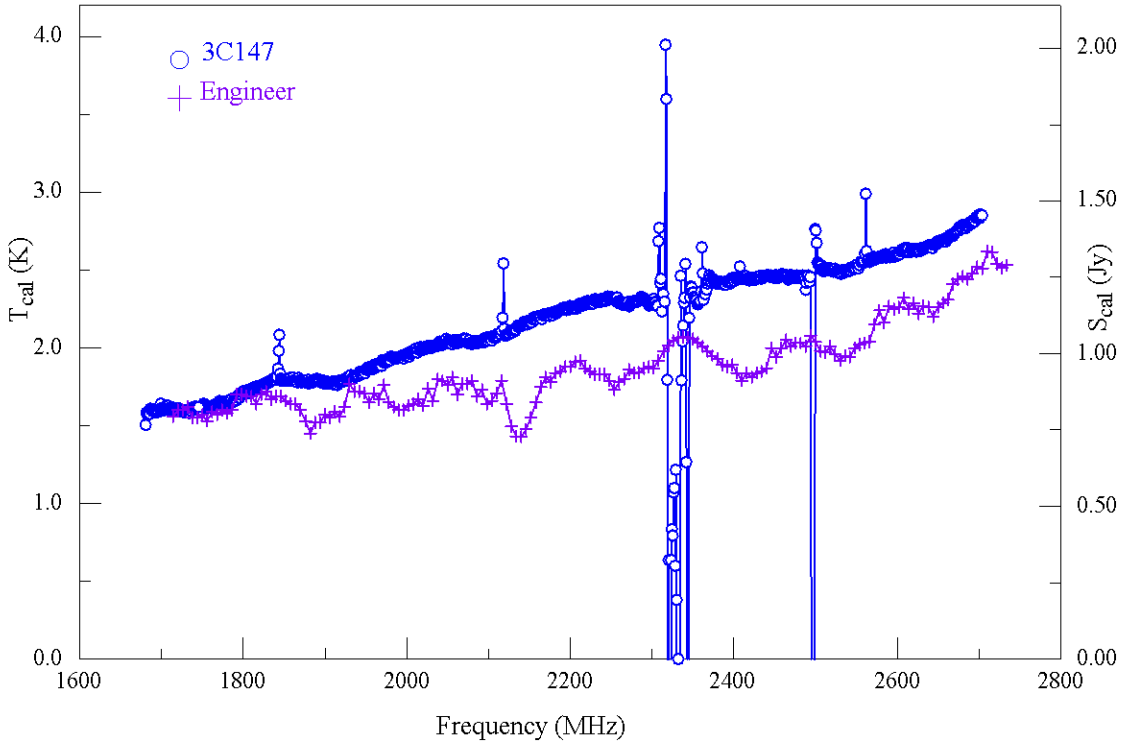

Figure 8. Y-Linear Polarization for the 2-3 GHz Receiver.

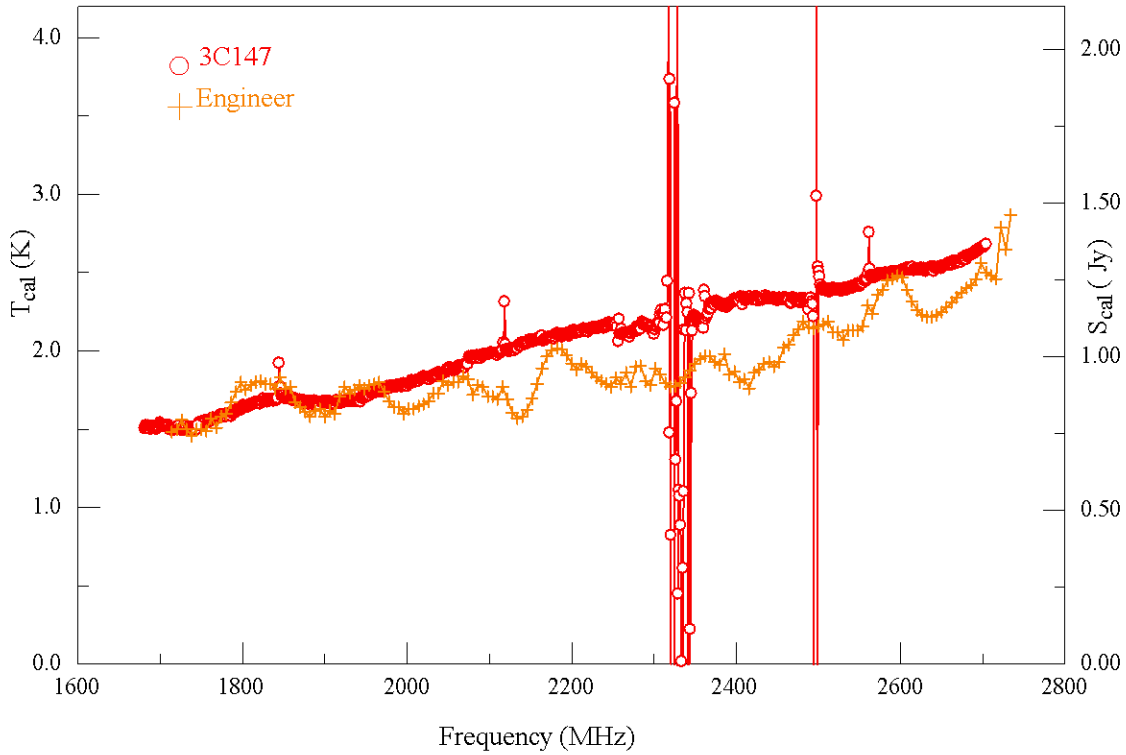

Figure 9. Left-Circular Polarization for the 2-3 GHz Receiver.

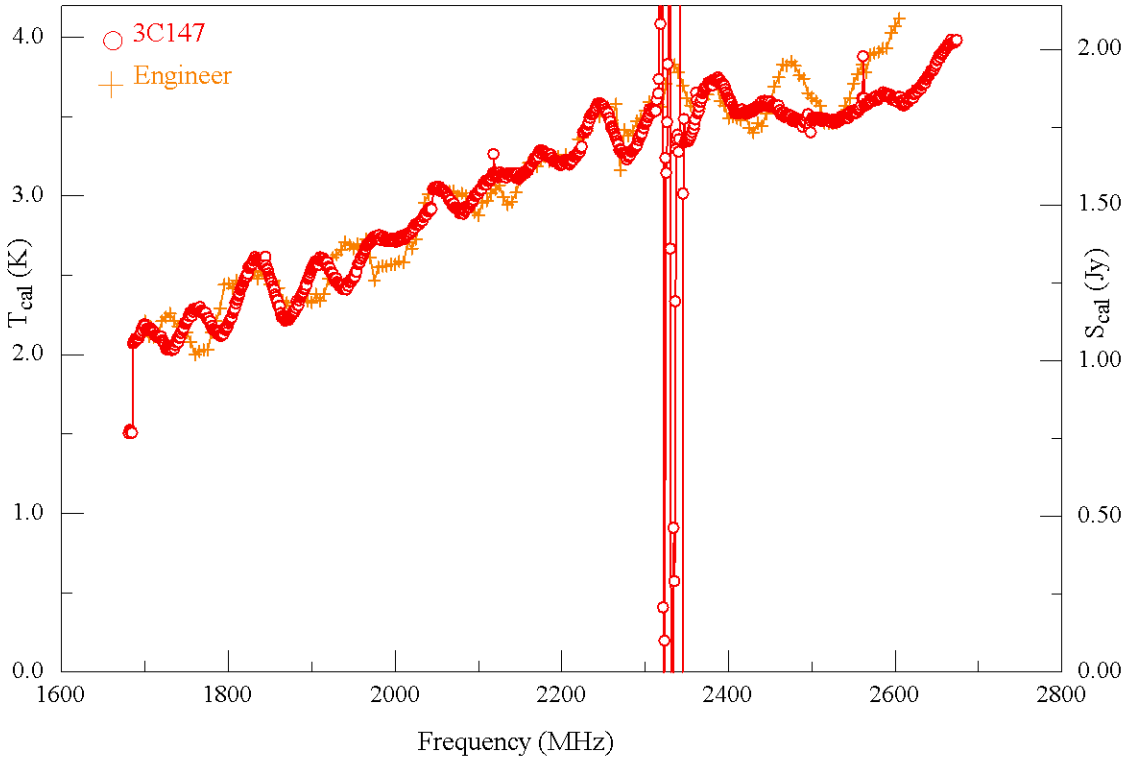

Figure 10. Right-Circular Polarization for the 2-3 GHz Receiver.

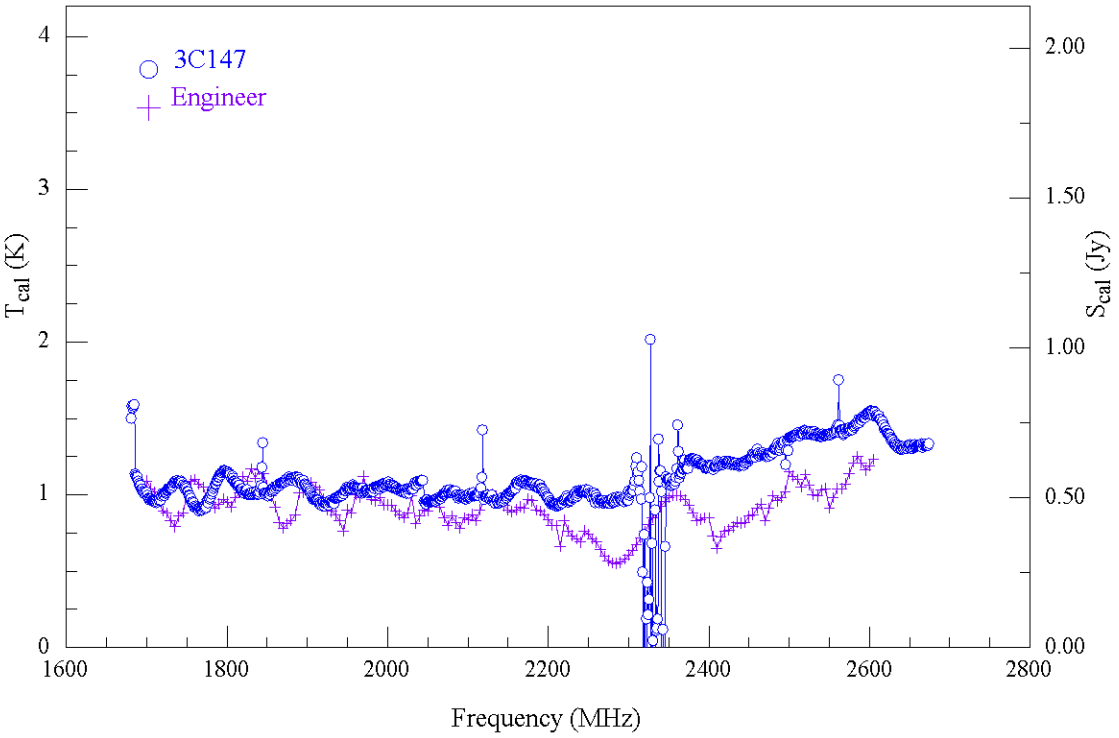

F. 4 – 6 GHz Receiver

As can be seen in figures 11 and 12, the astronomical calibration values for the 4-6 GHz receiver vary greatly. There are significant noise and interferences in the astronomical data, especially in the 4200 – 4270 MHz range, which could be attributed to commercial satellites (e.g., HBO), and in the 5600 – 5650 MHz range, which is an area of the spectrum devoted to air-traffic control. It should be noted, however, that pointing might have drifted during the observation so this may be a source of systematic errors within the 4-6 GHz data.

It may be worthwhile repeating the 4-6 GHz readings. At the time of this writing, the 4-6 GHz receiver was in the lab for repair. As such, these data could not be remeasured.

Figure 11. X-Linear Polarization for the 4-6 MHz Receiver.

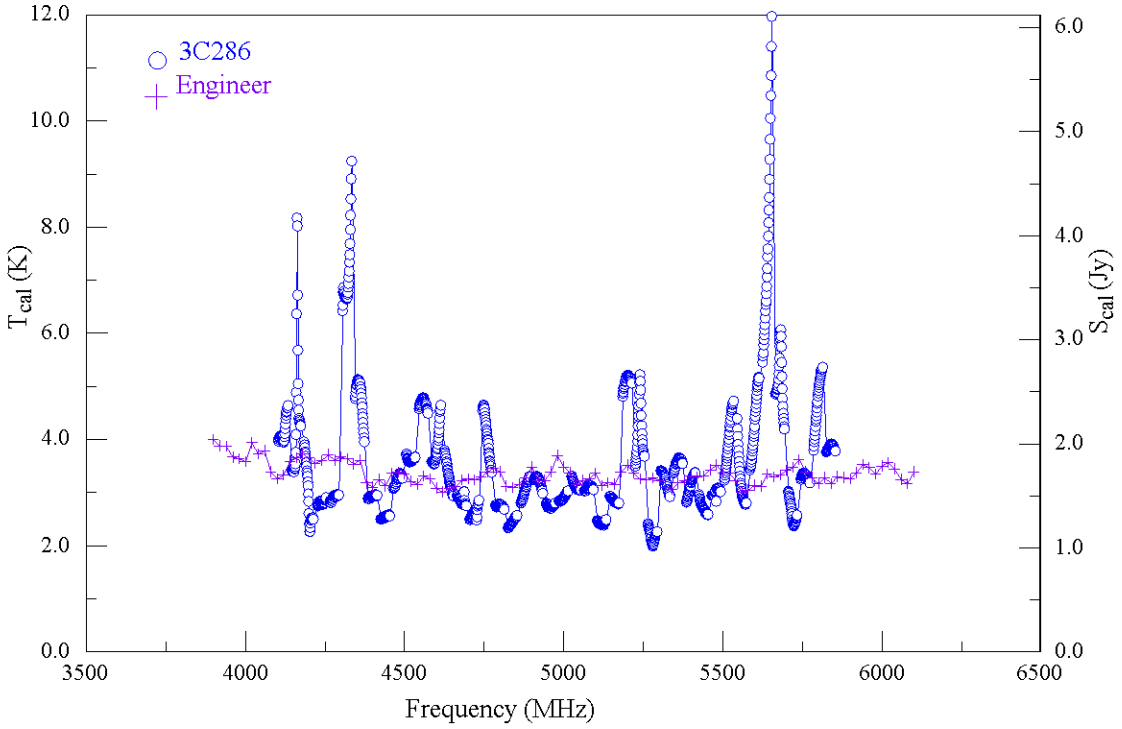

Figure 12. Y-Linear Polarization for the 4-6 GHz Receiver.

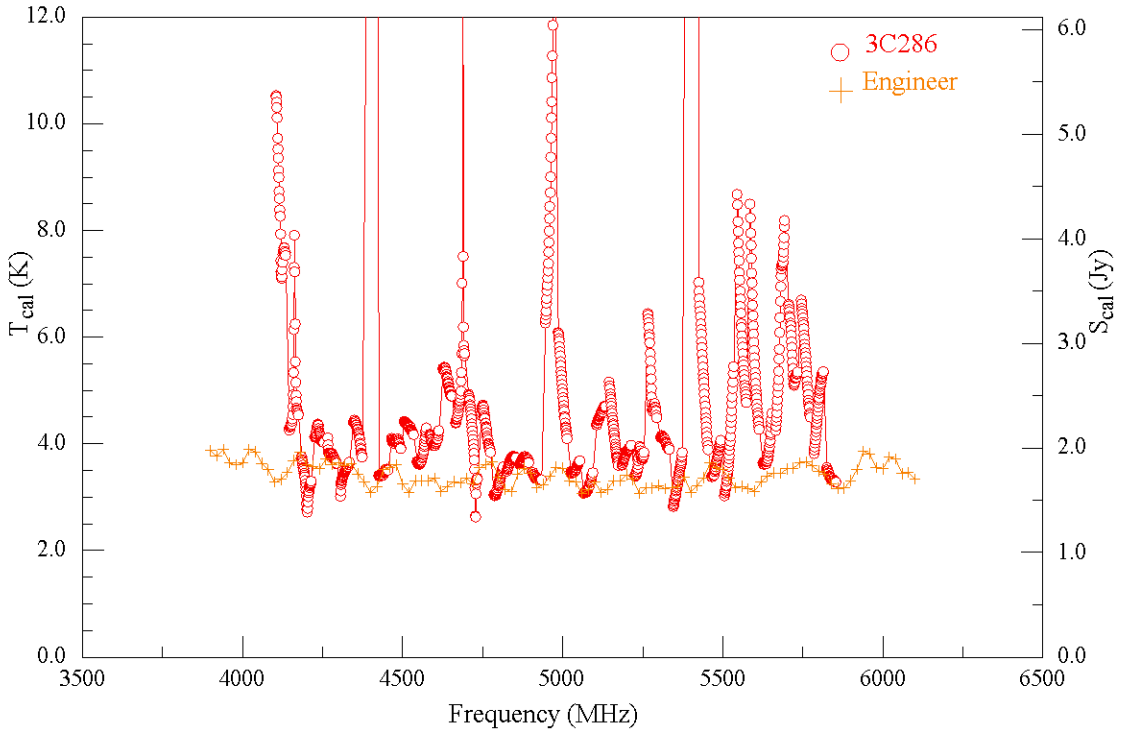

G. 8 – 10 GHz Receiver

As can be seen in Figures 13 and 14, the astronomical calibration values are slightly higher than the engineer's values. The slopes are similar. RFI does not seem to have contaminated any of the T_{cal} readings for the 8-10 GHz receiver. It should be noted, however, that pointing may have drifted during the observation so this may be a source of systematic errors within the 8-10 GHz data.

Figure 13. Left-Circular Polarization for the 8-10 GHz Receiver.

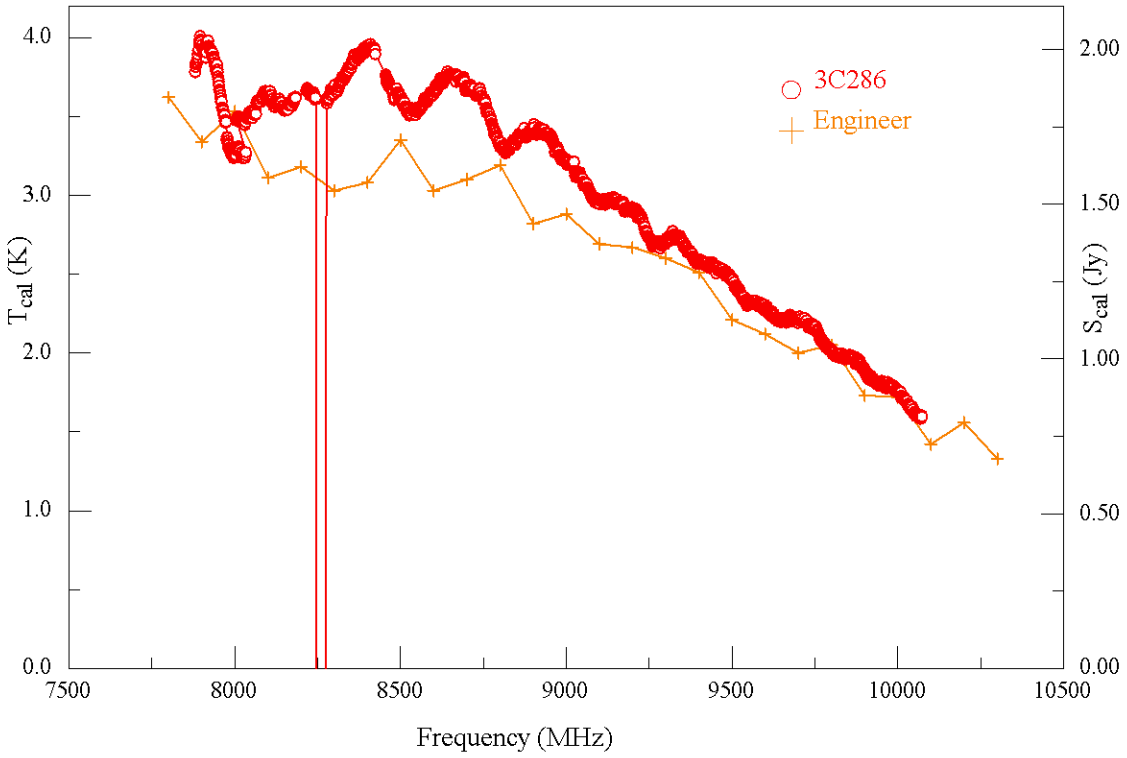

Figure 14. Right-Circular Polarization for the 8-10 GHz Receiver.

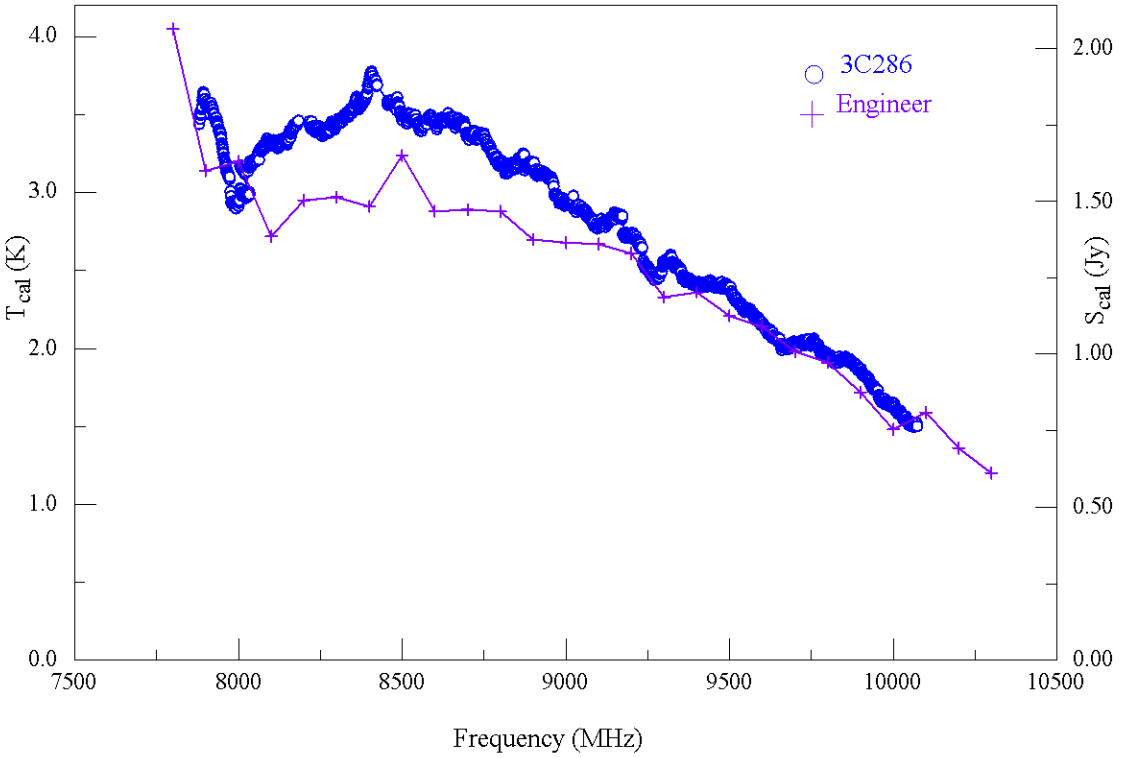

H. Conclusions

It is difficult to calibrate the low-end (less than 1300 MHz) of the 1-2GHz receiver due to prolific radio interference. The astronomical and engineer's linear polarization calibration values on the high-end of the 1-2 GHz receiver seem to agree within reason. It is important to note the excellent internal consistency of the method, with multiple runs generating T_{cal} values that agreed to better than 1%. Similarly, the 2-3 GHz T_{cal} values very closely agree with the engineer's values in both the linear and circular polarizations. The 4-6 GHz values are unusable; an additional calibration run would be helpful for comparison purposes. 8-10 GHz values are closely related with the engineer's values. All of the receivers suffer from RFI.

The astronomical observations take less time, less effort, and produce more repeatable and accurate results than the traditional engineer's methods. Unfortunately, astronomical observations cannot measure efficiency without knowing T_{cal}. To determine efficiency, we still require a few, high accuracy values of T_{cal} as determined by the engineer. Thus, a combination of astronomical measurements with a few lab measurements by the engineers might reduce total effort but with an increase in precision.

References

Baars, J.W.M.: 1973, IEEE *Trans. Antennas Propagation* **21**, 461.
Baars, J.W.M. et al.: 1977, *Astron. Astrophysics* **61**, 99.
Ott, M et al.: 1993, *Astron. Astrophysics* **284**, 331.
Roberts, M et al.: in preparation.
Tabara, H.: 1980, *Astron. Astrophysics Supp.* **39**, 379.

Appendix. Glish script used to calculate polarization values.

```
rsig := function  (val scan, val ns = 25) {
    numints := data_numints[ind(data_scannums)[(data_scannums == scan)]]

    vsigon := avrgrec(scan, 1, 2, numints)
    vsigoff := avrgrec(scan, 2, 2, numints)
    vrefon := avrgrec(scan-1, 1, 2, numints)
    vrefoff := avrgrec(scan-1, 2, 2, numints)
    vsig := combineOnOff(vsigon, vsigoff)
    vref := combineOnOff(vrefon, vrefoff)
    vsig.data.arr := (vrefon.data.arr - vrefoff.data.arr) / (vsig.data.arr - vref.data.arr)

    uniput("globalscan1",vsig)

    boxcar(ns)
    globalscan1 := uniget('globalscan1')
    a := getvfarray()

    for ( i in (1 : globalscan1.data.arr::shape[2]) ) print i, a.f[i], globalscan1.data.arr[, i];
    return T
}
```